Copyright © 1987, by the author(s).
All rights reserved.

Permission to make digital or hard copies of all or part of this work for personal or classroom use is granted without fee provided that copies are not made or distributed for profit or commercial advantage and that copies bear this notice and the full citation on the first page. To copy otherwise, to republish, to post on servers or to redistribute to lists, requires prior specific permission.

DETERMINATION OF PROCESS SIMULATION PARAMETERS FROM EXPERIMENT: PLASMA ETCHING AND PHOTORESIST DISSOLUTION

by

William R. Bell II

Memorandum No. UCB/ERL M87/47

30 June 1987

ELECTRONICS RESEARCH LABORATORY

College of Engineering
University of California, Berkeley
94720

DETERMINATION OF PROCESS SIMULATION PARAMETERS FROM EXPERIMENT: PLASMA ETCHING AND PHOTORESIST DISSOLUTION

by

William R. Bell II

Memorandum No. UCB/ERL M87/47

30 June 1987

DETERMINATION OF PROCESS SIMULATION PARAMETERS FROM EXPERIMENT: PLASMA ETCHING AND PHOTORESIST DISSOLUTION

by

William R. Bell II

Memorandum No. UCB/ERL M87/47

30 June 1987

ELECTRONICS RESEARCH LABORATORY

College of Engineering
University of California, Berkeley
94720

Determination of Process Simulation Parameters from Experiment: Plasma Etching and Photoresist Dissolution

William R. Bell II

ABSTRACT

Two I.C. fabrication process steps and the extraction of simulation model parameters for them are investigated. Plasma etching of tantalum polycide using chlorinated freons and sulfur hexaflouride is studied. It is shown that nearly vertical gate structures are achieved using these gasses, without the need for chlorine gas. Photoresist dissolution is also studied. A suite of software, PAREX, has been written which allows the automatic extraction of model parameters from experimental data gathered on a Perkin-Elmer Development Rate Monitor. An example using Kodak 820 photoresist developed in Kodak 809 is given, and the derived parameters are compared to previous characterization values. Lower values are found for high exposures, likely due to the lower level of agitation in the developer bath than in the previous measurement system. In addition, the surface retardation effect is much more difficult to extract due to noise in the data and it does not seem to be as pronounced possibly due to the lower level of agitation and to noise in the experimental data.

Acknowledgements

I would like to thank first and foremost my parents, and especially my father, who taught me to always strive to fulfill my potential. Without their encouragement and support, I know that I would not be where I am today. I would also like to thank Gino Addiego for his many hours of lively discussions on all aspects of life and even I.C. processing. Finally, I would like to express a deep appreciation to Professor Andy Neureuther who did all the right things.

This work was supported by industrial contributions under the California MICRO program (85-220), and Sandia National Labs (59-7419).

Chapter 1
Introduction

VLSI circuits have become increasingly more complex as the technology associated with them has matured. As the circuits become more complex, so does the technology required to fabricate them. In order that these processes can be made reliable and efficient, simulation has gained widespread use in their development. This has proved a useful tool in predicting results and interactions between various process steps. However, simulations are only effective when accurate models, based on experimental measurements, are used. Thus it is essential to be able to extract model parameters from experimental information. The extraction process must be efficient and reliable, as well as accurate and objective. It is these concerns that motivate the automation of this parameter extraction process. Objectivity is achieved by the removal of any biases which might be introduced by the interpretation by the individual experimenters. Efficiency is achieved by automating the procedure. Accuracy is improved by the ability to analyze a much larger amount of data than would be feasible by a hand analysis.

To this end, two I.C. fabrication process steps and extraction of simulation model parameters for them have been investigated. First, plasma etching of tantalum polycide is studied experimentally and critical issues for parameter determination are reviewed. Using key parameters, simulations are conducted and the results correlated with experiment. The focus of interest is on controlling the shape of the gate sidewall using chlorinated freons mixed with SF_6. Then, resist dissolution parameter extraction is studied, using a production monitor in a model parameter measurement mode. The emphasis is on the reliable determination of resist parameters under software control. Algorithms and special techniques are discussed, and results are compared to literature values. Finally, conclusions as to the effectiveness of the automation procedure are drawn, and suggestions are made for extension to other processes.

Chapter 2

Plasma Etching of Tantalum Polycide

2.1 Introduction

This chapter will discuss experimental and simulation work on etching tantalum polycide. This material is gaining widespread interest since, as integrated circuits become increasingly dense, the series resistance from polysilicon interconnect becomes more influential on the overall delay of the circuit. This situation has led to the investigation of other possible interconnect approaches such as a refractory metal layer over polysilicon gate, or polycide. This has the advantage of having a much lower series resistance than polysilicon alone while maintaining the relatively well understood interface of polysilicon and silicon dioxide for gate structures. In etching this two layer gate, it is desirable to produce sidewalls that are slightly tapered. Vertical sidewalls or undercut sidewalls tend to result in poor step coverage by an insulator. This in turn may lead to very poor subsequent metal coverage.

The motivation for this modeling study is to characterize this process for simulation in a multiple step process environment. The basic model used to advance the profile shape during the etching process requires the determination of the isotropic and anisotropic etch rates for each material. The ratio of these rates is determined from the anisotropy ratios observed experimentally using cantilever structures. This model is limited in the sense that it is necessary to observe at least one profile shape in order to simulate a profile rather than predict the profile shape from first principles. However, if the etch rates are constant throughout the process, it is possible to predict effects of process tolerances and surface topography.

The gasses chosen for the study were chlorinated freons in combination with SF_6. A homologous series of experiments have been planned using freon 13 (CF_3Cl), freon 12 (CF_2Cl_2), and freon 11 ($CFCl_3$). Studies have been performed using SF_6 with Cl_2, but the freons were chosen because they require less specialized equipment than the pure chlorine.

In addition, the freons are safer than Cl_2 and are less corrosive to the vacuum system. Finally, the freons are more readily available in the process flow. SF_6 was chosen as the base gas rather than CF_4 because the process has been shown to be less sensitive to the mixture of flourine and chlorine with the sulfur based gas. The nominal conditions for the experimental matrix were chosen based upon the results of the study by Mattausch et al[1] and are shown in Table 2.1 It has been hypothesized that collisions in the plasma result in complete dissociation of the gas molecules. Based upon this, the nominal gas mixture (ratio of SF_6 to CF_2Cl_2) was chosen simply by taking the optimal mixture from Mattausch et al[1] and matching overall atom counts.

2.2 Experimental Characterization

2.2.1 Apparatus

The etcher used in these studies is a 12" Plasma-Therm parallel plate reactor. A schematic of the reactor is shown in figure 1. The rf power can be applied to either electrode to etch in either RIE or plasma mode. All the experiments in this report were conducted with the etcher in RIE mode, i.e. with the lower elctrode powered. The 4" wafers were prepared by Sandia National Labs (from Ron Light) in the following way. After growth of a 100 Å thermal SiO_2, a 2500 Å layer of polysilicon was deposited, and a 2500 Å layer of $TaSi_{2.5}$ was then cosputtered on the top. $TaSi_{2.5}$ was used instead of $TaSi_2$ because of its better adhesion to polysilicon. Lithography was performed using 1 μm Kodak 820 photoresist exposed using a GCA 6200 projection printer. The photoresist was postbaked for 30 min. at 120°C to be more etch resistant. After lithography and the postbake, the wafers were then broken into 1 cm^2 pieces, so that loading effects in the etch process were avoided and fewer wafers were needed.

2.2.2 Experimental Matrix

An experimental matrix was designed to investigate the effect of the process from varying different parameters. This is a 7 dimensional matrix with the dimensions being:

chlorinated gas molecule, mixture, flow, time, power, pressure, and temperature. Not all of the dimensions have been fully investigated yet, however. In the work described herein, a set point consisting of constant gas, power, flow, and pressure was chosen in order to reduce the dimensionality of the experimentation. These dimensions will be investigated in further work. In addition, temperature has only been seen to have an effect upon the initial etch. If the wafer is initially at a low temperature, the plasma heats it up until by the end of the etch, it has reached the higher set point. Thus the system is self consistent to the extent that it always reaches approximately the same temperature.

Experimental Matrix

Parameter	Allowed Values		
	Minimum	Nominal*	Maximum
Gas	CF_3Cl	CF_2Cl_2	$CFCl_3$
Mixture	$20SF_6$	$12SF_6/8CF_2Cl_2$	$20CF_2Cl_2$
Flow	10 sccm	20 sccm**	40 sccm
Time	0 min.	4:30 min.	6 min.
Power	250W	350W	450W
Pressure	20mT	40mT	100mT
Temperature	20°C	70°C	100°C

*Note: Nominal Parameters are interdependent.
**Note: See comment in text below regarding flow.

2.2.3 Results

Two sets of experiments were run. A gross matrix was run initially to verify the set point and the trends as mixture was modified. These are indicated as Samples 1, 2, and 3 (Shown in figures 2, 3, and 4). Sample 1 was etched using the nominal etch conditions, and it shows the desired sidewall shape. However, it is possibly overetched. Sample 2, on the other hand is very badly overetched. This sample yields very little useful information, yet points out a potentially serious problem, that of "grass" growing on the wafers and chamber. This grass may be due to nonvolatile sulfur polymer and could have signifcant effects upon the chamber in the long term. Sample 3 yields better results. It is also overetched, as can be seen by the step below the polysilicon, where the oxide was broken through. It also indicates that there is significant ion bombardment occurring. This is demonstrated by the erosion of the underside of the resist, due to ions reflected up off the

substrate.

The second set of experiments consisted of a finer matrix in an attempt to fine-tune the process and investigate reproducibility. This set consists of Samples 4, 5, and 6 (Shown in figures 5, 6, 7, and 8). Sample 4 was again etched under the predicted nominal conditions. this time, however, it does not yield the ideal results obtained with sample 1. It shows undercutting of the polysilicon along the right side of the SEM. Also, it may now be slightly underetched, since the height of the etched area is only 0.36 μm. Sample 5 was etched with slightly more SF_6 than sample 4. It shows no discernible discontinuity between the silicide and polysilicon layers. However, as seen in figure 7, a significant amount of surface roughness is evident, indicating again that ion bombardment is very involved in the etch. Finally, sample 6 was etched with slightly less SF_6 than sample 4, yet it shows a drastically different profile. Here again, ion bombardment plays a large role, indicated by the surface roughness and the undercutting of the resist. In addition there is a large lateral etch rate indicating that ion bombardment is not the only process.

Experimental Settings

Sample	Mixture(SF_6/CF_2Cl_2)	Time	Temperature
#1	11/8	4:30	70°C
#2	16/4	4:30	70°C
#3	6/14	4:00	70°C
#4	11/9	3:00	20°C
#5	12/8	3:00	20°C
#6	13/7	3:00	20°C

The process is seen to be sensitive to both mixture and time. There are several contributors to this effect. First, the flow was set to be 20 sccm (standard cubic centimeters per minute). However, due to a miscalibration of the mass flow controllers, the actual flow was twice that, or 40 sccm. In addition, the power input to the system was the variable used, while the actual parameter of interest is power **density**. If the size of the electrodes used in reference[1] is very different from the size of the electrodes used in this work, then simply using input power is not valid. This could explain the drastic overetching which is seen in samples 2 and 6 (Figures 3 and 8). It is expected that better etching selectivity will be seen with lower power settings.[2] In addition, substantial surface damage can be

seen on sone of the samples, which would suggest that they are being subjected to significant ion bombardment. This is shown in figure 7. Overall, the same trends as seen in reference [1] are seen here. This would indicate that chlorinated freons are acceptable gasses for this process.

Finally, another possible cause for the sensitivity of the system is the interaction of the carbon, chlorine and flourine. It has been shown that depending upon their relative concentrations, two different effects can occur.[2] First, if the chlorine concentration is low, the freon may release chlorine and react with F to form related freons. This has the effect of reducing the relative F concentration and thus increasing anisotropy and the etch rate of the polysilicon. However, as the Cl concentration is increased, thermodynamically less favorable reactions begin to occur, which remove Cl and release F, thereby increasing isotropy and reducing the etch rate of the polysilicon. This is seen in figure 8. By using the freons instead of Cl_2, the ability to independently set the relative concentrations of Cl and F may be lost, due to the uncertainty in what species will be created by the fragmentation of the molecules in the plasma. However, the current results suggest that this is not an insurmountable problem.

2.3 Simulation of the Process

In addition to the experiments conducted, a simulation study was also performed. The rates for this study were generated using rate versus mixture graphs in Mattausch et al.[1] This graph is shown in figure 9. The degree of anisotropy was estimated from the pictures of the results. The results from the simulation show very good agreement with the results shown in the reference. Both simulation results and experimental results from the reference are shown in figures 10, 11, and 12. As can be seen they match very closely. The inputs for the simulations are given in Appendix A.

This study shows that simulation parameters can be extracted easily from common experimental procedure, namely examining the etch rate. The only improvement that would be suggested is that anisotropy curves should also be included. This would alleviate

the problem of having to estimate the degree of anisotropy from the pictures.

In addition to correlating the simulations to the literature, the simulations were also compared to the earlier experimental results. Again, good similarity was demonstrated. This is very encouraging and shows that basic characterization of the process is sufficient to fully describe it for simulation purposes.

Chapter 3
Photoresist Dissolution

3.1 Introduction

A second and more extensive example of generating model parameters for simulation is the determination of resist parameters from dissolution data. For this effort to be efficient and reproducible, it should be automated as much as is possible. In this way, various random influences may be removed, such as operator bias to a certain extent. To this end, a suite of software, called PAREX (PARameter EXtractor), has been developed to analyze dissolution rate versus thickness data and extract the parameters for generating rate R versus exposure state M plots. A flow chart for the software is shown in figure 14. The software suite also includes algorithms for SAMPLE to generate M versus depth.

In the broadest view of the problem, the algorithm to extract the parameters is fairly simple. First, conduct experiments and collect rate versus thickness data. Then simulate the exposure process using SAMPLE in order to generate M values. Next, associate an M value with each rate-thickness pair based upon the depth. This will result in a matrix of rate and M versus depth. This data can then be used by a curve fitting program in order to fit the data to the model. This curve fitting process can use any appropriate algorithm, including a least squares method. In our case, we use a modified least squares approach which uses a Jacobian and the Marquardt condition to predict the deepest descent.

The experimental apparatus used in the development of this software was a Perkin-Elmer Development Rate Monitor (DRM). This system measures reflectivity versus time and determines thickness versus dissolution time for photoresist which has been spun onto reflecting substrates, such as those commonly used in the process line. This is in contrast to other systems, which require specialized substrates. The experimental data is collected and initially analyzed using DREAMS, a software system written by Perkin-Elmer for the DRM. DREAMS analyzes the data to generate thickness versus time. the experimental data used herein was generated using DREAMS version 1.0. The data is then input to

PROSIM (version 1.0) to generate rate versus thickness from the thickness versus time data. The methodology used is not dependent upon any particular aspect of the DRM, and could easily be modified to manipulate data generated using a different experimental apparatus.

In this chapter, the theory of photoresist dissolution upon which this work is based will be presented,[3] in order to lay a foundation for the discussion of the methodology. The presentation will not be extensive, however, and for a fuller treatment, references [3,4] and[5] should be consulted. Then a description of the experimental apparatus will be presented, so that the essential features can be understood and system requirements can be identified, with the intention of extension to include other systems in the future. Again, this will be a brief description and the manufacturers documentation should be referenced in order to obtain a complete understanding of the system. Finally, a discussion of the methods used to extract the model parameters from the experimental data will be given. In addition to the method used here, one other method will be briefly presented, and potential obstacles of each method will be identified.

3.2 Background

3.2.1 Theory

Optical microlithography can be separated into several independent sub-steps: imaging, exposure and development. This work is concerned with characterizing the final dissolution step. Optimizing lithographic performance depends on balancing complex interrelationships between these steps. The imaging and exposure steps are connected through the intensity of energy incident upon the photoresist surface. The imaging system defines the local intensity at any position across the wafer, which then determines the local incident energy across the wafer. The exposure bleaching determines the local dissolution rate and simulation is best used for understanding the interrelationship.

Photoresist consists of several materials, most importantly the photo-active com-

pound (PAC). In a positive resist, this is the material which bleaches during the exposure process into photo-produced acid (PPA). This PPA containing area is then dissolved away during the development procedure. The photoresist's exposure state is described by specifying a value M which is the normalized concentration of PAC. This is defined to be 1.0 before exposure, and 0.0 in a completely bleached resist.

The value of M at any location in the resist prior to development depends on a number of factors. It depends on physical parameters of the resist which describe its absorption of energy as well as the total energy incident upon the surface. In addition, it depends upon the characteristics of the underlying layers, such as the thickness and refractive index (which is often wavelength dependent), because these can interact to create standing waves of energy in the resist and thus periodic variations in the value of M.

The motivation for using this parameter to describe the state of the resist is that the dissolution rate is a a function of M alone, in the simplest case. The exposure creates a variation of M in the resist and the local value of M then determines the local dissolution rate. By associating a value of M with each rate value, it is possible to then fit the resist's behavior to a model.

The difficulty with this picture is that M is not easily measurable and thus is generally calculated from the exposure conditions and the material parameters. This in itself can be a difficult task. As a result of the wave nature of electromagnetic energy, if the indices of refraction, at the wavelength of the energy, of the various layers are different, reflection from the interface occurs. This reflection will cause standing waves of energy in the resist and thus the shape of the distribution of M will not in general be simple, although it is often sinusoidal. This variation of M with depth is shown in figure 13. If the index of refraction of the substrate is very close to that of the resist ("matched"), the energy envelope will not be generated, and the distribution of M will be monotonically increasing into the resist. In this situation, it is relatively easy to relate the distribution of M to deposited energy.

In general, though, this is not the case. For example, silicon is a reflecting substrate and large standing waves can be produced. Since silicon is used extensively in I.C. production, it would be advantageous to be able to measure dissolution properties of photoresist on these substrates. This is the focus of this work. The DRM gives one the ability to measure dissolution rates on a variety of substrates, including silicon, and this software enables the interpretation of this data.

3.2.2 Discussion of the Experimental Apparatus

A brief description of the DRM is now in order. The DRM projects a filtered, narrow band, collimated beam of light, with λ_{meas} = 633nm., onto the surface of a wafer which is immersed in a development tank. This laser is reflected off the moving resist surface and the stationary substrate during development, and the resulting interference signal is received by a photodiode array. This allows the simultaneous measurement of multiple exposure doses under the same development conditions. This is a tremendous advantage, since an order of magnitude more exposure doses can be measured at once. This signal is then analyzed by the DREAMS software using the knowledge that interference fringe maxima will be separated by $\lambda_{meas}/2n_{meas}$ to generate thickness versus time data. This data is further analyzed in PROSIM, by a process involving differentiation, to create rate versus thickness data within the DRM. The rate versus thickness data is the starting point for the manipulation of the data in our software suite to determine R(M,z). The data is then transferred to a VAX using the communications capabilities of the Idris operating system on the DRM. For a more complete discussion of the DRM and related software, consult references [6] and 7.

3.3 Extraction Algorithms

In this section, the algorithms used to determine the model parameters from the rate versus thickness parameters will be discussed. The algorithms presented have been designed to be general enough so that, first, any apparatus available could be used to gen-

erate the experimental data, and second, that this data could be fit to whatever model is desired. The flow of the data analysis will be discussed first in order to give a feeling for the intent of the project. Then the difficulties in the procedure as well as the current implementation will be discussed.

3.3.1 Usage of the Parameter Extraction Software

Figure 14 shows a flow graph of the PAREX software which has been developed. The DRM is used to conduct the experiment, and the data is initially analyzed using the Dreams software package developed by Perkin-Elmer. Then Prosim is used to generate the rate versus thickness data from thickness versus time. This data is then transferred from the DRM to a larger computer where the rest of the parameter determination procedure is conducted. There is no inherent reason why the software could not run on the DRM, but currently it is more convenient to use a larger machine. At this point, the data can be represented by the file R(z) shown on the figure. This data is then input to FINDRM, where the rate versus thickness values are correlated with the M values. The box marked SAMPLE represents that the exposure module from SAMPLE is incorporated into FINDRM. FINDRM then outputs a file consisting of rate versus M versus depth, which is in turn input to RPARM. It is in RPARM that the parameters are actually fit to the data. The output from RPARM is the parameter values.

In addition to the software written for the data analysis, a set of filters and programs were written to view the data graphically at various points in the analysis. These filters take the information and prepare it for another tool, PLOTTER. This program is a general purpose plotting package. PLOTRZ allows the data from the DRM to be inspected before being processed. After the data has been processed by FINDRM, it can be viewed using PLOTRM, which shows the rate versus M value for all the data. PLTBLK shows rate versus M with the surface stripped off. Also, PLOTRANM shows the rate and M versus depth, so that the rate and M can be inspected with respect to each other. After the data is fitted to the curve in RPARM, PLOTDT takes the R(M,z) file and correlates it

with the calculated parameters. It then prints the experimental data with the model data so that the fit can be visually inspected.[8]

3.3.2 Some Specific Details

3.3.2.1 General Concerns

There are two categories of obstacles included here. First, there are general difficulties associated with the algorithm, and then there are difficulties which relate to our implementation.

First, the general problems. On reflecting substrates, the standing waves create a variation in M with depth and thus a variation in rate. Ideally, if these are in phase, they will show a linear fit when plotted against each other.[8] This can be seen in figure 15. However, if they are out of phase, a spread in the data will result which will make the subsequent step of fitting the data to the model very difficult and slow to converge. This is assuming that it can converge to the correct value, since the mismatch can alter the data dramatically. Because of the small period of the standing waves (period = $\lambda_{exp}/2n_{exp} \approx$ 130nm.), even a small experimental error in the calculation of the thickness can result dramatic variations in the rate versus M data. This variation of rate versus M as a function of depth can be considered to be similar to the Lissajous patterns seen on oscilloscopes and seen in figure 16.[8] Thus it is important to match the phase of the two sinusoidal signals.

In addition to a lateral shift to a thickness error, a second problem is the difference in the period between the measured and simulated data. The model assumes that rate is a function of M, and the periodic variation in M implies a periodic variation in rate. Thus the period of the two curves, rate and M versus depth, should be the same. An inaccuracy in the value of n_{exp}, the index of refraction at the exposure wavelength, will result in different periods in the two curves. This can be countered by calculating an effective index, n_{eff}, from the periodicity of the rate data, and using that value in the simulation of

M.

The difference in the value of n which is measured using a different experiment, and n_{eff} from the rate data, could be due to several factors. One of the primary ones is that to calculate thickness versus time, one must know the measuring wavelength, λ_{meas}, and the index of refraction at the measurement wavelength, n_{meas}. This is because the peaks in the recieved interference signal are spaced $\lambda/4n_{meas}$ apart.[6] Thus an error in the value of n_{meas} will modulate the thickness versus time curve and thus the period of the rate versus thickness curve, thereby creating an n_{eff} which is different from n_{exp}. Also, if the beam of light is not incident normal to the surface, the path length of the reflected beam will change and an error in the period of the thickness versus time data will be created.

Finally, a third problem is that the mere act of generating rate versus thickness from thickness versus time is a potential source of noise induced errors. This procedure involves taking a numerical derivative, which is very sensitive to noise in the data. It requires sophisticated filtering techniques to remove this noise and generate reasonable data. Even after it is smoothed, the concern is whether or not the data is still valid. Has it been corrupted by all the manipulation that it has undergone? This is a difficult question to answer, and leads one to investigate other possible algorithms.

One very promising approach is to avoid the difficulty associated with taking this numerical derivative and use the thickness versus time data to fit to the model.[9] The algorithm is simply as follows. Generate the thickness versus time data, and simulate the M versus depth information. Now, estimate the rate parameters, and using the exposure information, calculate the resulting thickness versus time profile using those parameters. Compare this curve with the experimental curve to define an error function and then modify the estimated parameters to minimize the error. This approach has the disadvantage that experimental data points for dissolution rate versus m are not generated.

3.3.2.2 Concerns Particular to the DRM Implementation

The primary concern which is caused by our desire to determine resist model parameters has to do with the quality of the rate versus depth data. The conversion from thickness versus time to rate versus thickness in our system is done by PROSIM, a program from Perkin-Elmer.[10] PROSIM is a PROfile SIMulator which uses the experimental data to simulate microlithographic profiles. Because of their application, their motivation in manipulating the data is slightly different from ours and this is where the "conflict" arises. For example, for profile simulation in PROSIM all of the rate data for various exposures is corrected to correspond to a uniform thickness. However, data for each individual exposure shows a thickness variation due either to the DREAMS analysis algorithms or to actual variation on the wafers. Therefore, it is necessary to filter their data in order to remove the false points that have been added by PROSIM. To avoid Lissajous figure spread in determining resist model parameters it is necessary to use a different resist thickness for each exposure dose.

A second problem encountered in the data from PROSIM is that the minimum rate does not always occur at the resist silicon interface. This may be due to physical effects such as the presence of an oxide layer or large molecules in the resist leaving a scum which is difficult to remove. It may also be due to the algorithm by means of which the rate versus thickness is determined. In simulation, an oxide free interface is assumed and it is necessary to remove the data beyond the rate minimum.

3.4 Parameter Determination Results

To illustrate the parameter extraction process and the results obtained, an example will be presented and discussed at the various stages in the analysis. This example is of Kodak 820 photoresist with Kodak 809 developer on a silicon substrate. Figure 17 shows a sample set of rate versus depth data for this system. This data has been taken directly from the DRM. It consists of 100 equally spaced points, and shows some noise, but not an intolerable amount.

This rate data is then used in FINDRM, and figure 18 shows a plot of rate and M versus depth. An n_{eff} is calculated for the rate versus thickness data and then used in the simulation of M versus depth. As can be seen, the periods of the two curves match reasonably well, showing that the n_{eff} is a valid model to use. The same data can be plotted in the form of bulk rate versus M. The spread in the data is due to the phase error resulting from the substrate interface not being an energy minimum. This causes the desired linear match as seen in figure 15 to spread into the cloud seen in figure 19.

The entire set of data can also be viewed (figure 20). In this case the data is spread out, not only due to the phase error, but also due to the surface inhibition effect seen for this resist.

Finally, figure 21 shows the experimental and the fitted data together. The extracted parameters show a good correlation with the experimental data. These parameters are shown in table 3.1 in the column labeled Bell.

Table 3.1

Parameter	Bell	Kim	
R_1	0.0364	0.23	μm/sec
R_2	0.00174	0.0016	μm/sec
R_3	3.32	5.6	
R_4	0.024	0.25	μm
R_5	0.4933	0.62	
R_6	0.268	0.08	

Table 3.1 also shows the parameters derived herein compared to previously extracted values using a different experimental apparatus.[11] These two sets of parameters are shown together in figure 22. The much lower R_1 value calculated herein fits the current experimental data and suggests that in the DRM system, for low values of M the dissolution rate is probably transport limited rather than reaction rate limited as in Kim's apparatus, which used very high flow rates for the developer. Some of the other variances are probably due to the phase shift induced error as shown in figure 18. The value of R_4 is also much smaller than observed previously. This may demonstrate that the surface retardation effect is not seen for developer systems with low flow rates, or that the noise in the rate versus thickness data may be masking the effect. It is considered that the second effect is

more likely, and will be treated in future work.

Chapter 4

Conclusion

Two of the processes that are used in I.C. fabrication and the extraction of simulation model parameters for them have been investigated. Plasma etching of tantalum polycide using chlorinated freons mixed with sulfur hexaflouride. It has been shown that nearly vertical gate structures can be achieved without using Cl_2. In addition, the process has been simulated using data from the literature.[1] The standard characterization of the process, consisting of etch rate data for each layer, has been shown to be sufficient to model the process, provided the degree of anisotropy is included.

For photoresist dissolution, a software suite, PAREX, has been written to automate the parameter determination process. A program, FINDRM, was written which successfully correlates simulated values of M with experimental values of rate versus thickness. This program corrects for apparent thickness variations between zones, and also matches the effective refractive index of the photoresist so that the best match with the M values can be achieved. Another program, RPARM, was written which uses the rate versus M versus depth data and fits it to a desired resist model. This procedure has been shown to be effective and to yield reasonable results comparable to those of Kim on matched substrates. The variations in the parameters, such as the lower dissolution rates at high exposure, appear to be due the lower level of agitation in the DRM system versus Kim's high flow rate system. The less pronounced surface retardation effect is suspected to be due to a masking effect due to noise. Future effort will emphasis reduction of the noise in the data. In addition, parameter determination by fitting to thickness versus time data directly has been shown to be plausible.

References

1. H. J. Mattausch, B. Hasler, and W. Beinvogel, "Reactive Ion Etching of Ta-silicide/polysilicon double layers for the fabrication of integrated circuits," *J. Vac. Sci. Technol. B*, vol. 1, no. 1, pp. 15-22, Jan.-Mar. 1983.

2. H. H. Wang, "Plasma Etching of Poly in $SF_6 + Cl_2$ Mixtures," *Proceedings of the 3rd Intl. Symposium on VLSI Science and Technology: VLSI Science and Technology/1985*, vol. 85-5, pp. 316-325, The Electrochemical Society, 1985.

3. F. H. Dill, W. P. Hornberger, P. S. Hauge, and J. M. Shaw, "Characterization of Positive Photoresist," *IEEE Trans. Elec. Dev.*, vol. ED-22, pp. 445-452, July 1975.

4. F. H. Dill, "Optical Lithography," *IEEE Trans. Elec. Dev.*, vol. ED-22, no. 7, pp. 440-444, July 1975.

5. D. J. Kim, W. G. Oldham, and A. R. Neureuther, "Development of Positive Photoresist," *IEEE Trans. Elec. Dev.*, Dec. 1984.

6. A. W. McCullough and S. P. Grindle, *Resist Characterization Using a Multichannel Development Rate Monitor*, Perkin-Elmer Corporation, May 1984.

7. *DRM/Dreams Operator's Manual for Model 5900*, Perkin-Elmer Corporation, 1984.

8. John Hayes, William R. Bell II, Richard Ferguson, and Andrew R. Neureuther, "Resist Characterization on Reflecting Substrates," *Proceedings of SPIE: Advances in Resist Technology and Processing III*, vol. 631, pp. 8-13, March 1986.

9. Chris A. Mack, March 1986. Personal Communication

10. *DRM/Prosim Operator's Manual for Model 5900*, Perkin-Elmer Corporation, March 1986.

11. D. J. Kim, *Characterization and Modeling of Positive Photoresist*, Electronics Research Lab UCB, 17 August 1984. No. UCB/ERL M84/65

Appendix A:
SAMPLE Input Files

```
# SAMPLE input file for figure 10.
#
# Dir. etching of poly-Si on oxide.
# Iso/aniso etch rate pairs.
trial 78 10 0.0001 0.0002  # resist (15:5 SF6:Cl)
            0.0000 0.0015  # Ta-Si2
            0.0053 0.0013  # poly-Si
            0.00   0.00    # oxide
            0.00   0.00  ; # substrate
trial 79 -3 5            ;
trial 79 4 1.0           ;
trial 79 3 0.20          ;
trial 79 2 0.30          ;
trial 79 1 0.04          ;
trial 79 0 0.46          ;
trial 84 10              ;
trial 85 0.0 1.0 0.8 1.0
         1.0 0.2 1.2 0.0
         2.8 0.0 3.0 0.2
         3.2 1.0 4.0 1.0
trial 86 4.0             ;
trial 87 1 1             ;
trial 88 30 180 6        ;
trial 89                 ;
```

```
# SAMPLE input file for figure 11.
#
# Dir. etching of poly-Si on oxide.
# Iso/aniso etch rate pairs.
trial 78 10 0.0001 0.0002        # resist (12.5:7.5 SF6:Cl)
            0.0010 0.00033       # Ta-Si2
            0.0020 0.0055        # poly-Si
            0.00   0.00          # oxide
            0.00   0.00    ;     # substrate
trial 79 -3 5                  ;
trial 79 4 1.0                 ;
trial 79 3 0.20                ;
trial 79 2 0.30                ;
trial 79 1 0.04                ;
trial 79 0 0.46                ;
trial 84 10                    ;
trial 85 0.0 1.0 0.8 1.0
         1.0 0.2 1.2 0.0
         2.8 0.0 3.0 0.2
         3.2 1.0 4.0 1.0
trial 86 4.0                   ;
trial 87 1 1                   ;
trial 88 200                   ;
trial 89                       ;
```

```
# SAMPLE input file for figure 12.
#
# Dir. etching of poly-Si on oxide.
# Iso/aniso etch rate pairs.
trial 78 10 0.0001 0.0002  # resist (10:10 SF6:Cl)
            0.0022 0.00    # Ta-Si2
            0.0001 0.0076  # poly-Si
            0.00   0.00    # oxide
            0.00   0.00  ; # substrate
trial 79 -3 5              ;
trial 79 4 1.0             ;
trial 79 3 0.20            ;
trial 79 2 0.30            ;
trial 79 1 0.04            ;
trial 79 0 0.46            ;
trial 84 10                ;
trial 85 0.0 1.0 0.8 1.0
         1.0 0.2 1.2 0.0
         2.8 0.0 3.0 0.2
         3.2 1.0 4.0 1.0
trial 86 4.0               ;
trial 87 1 1               ;
# Set the times
trial 88 30 350 5          ;
trial 89                   ;
```

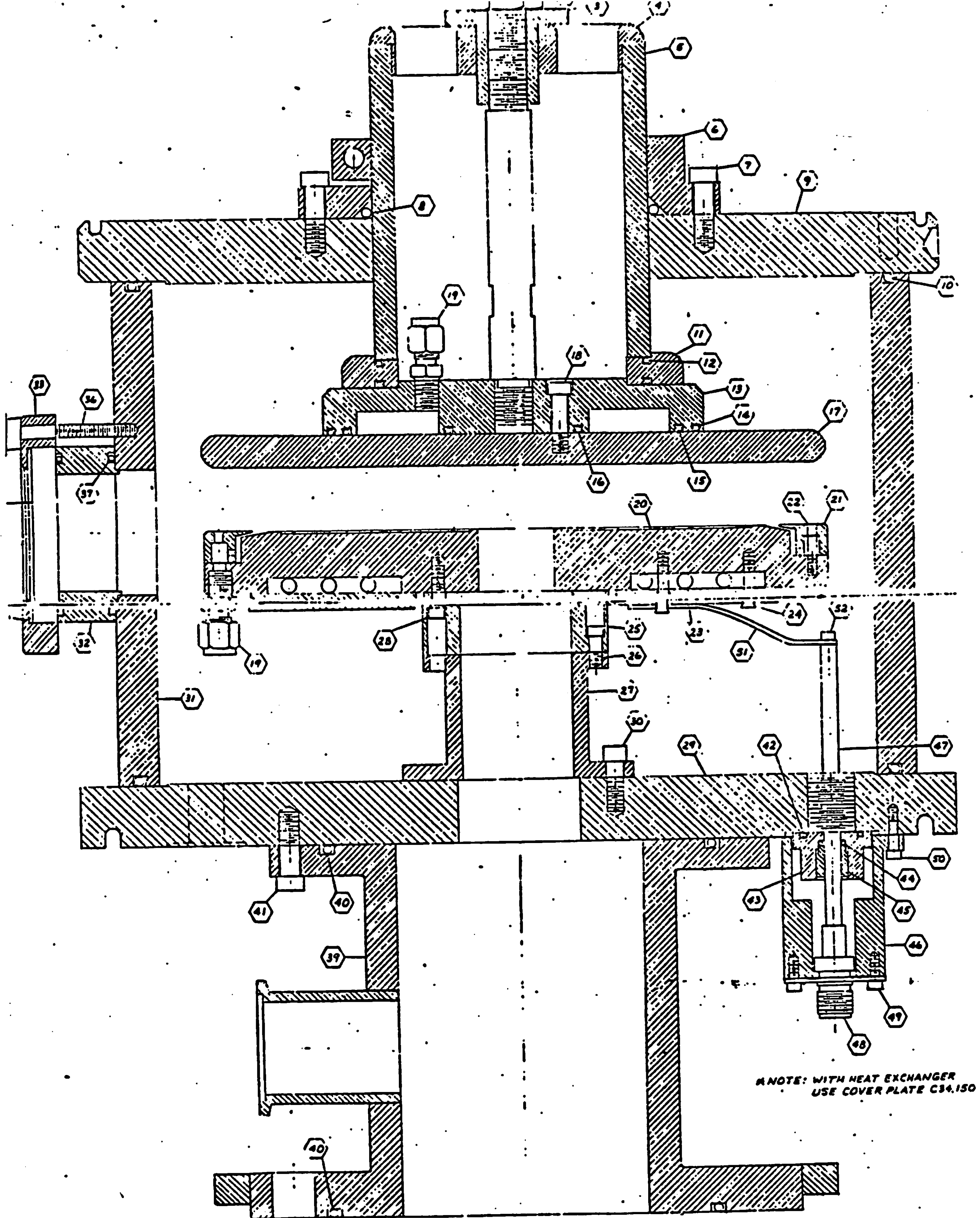

Figure 1. Schematic diagram of Plasma-Therm plasma reactor.

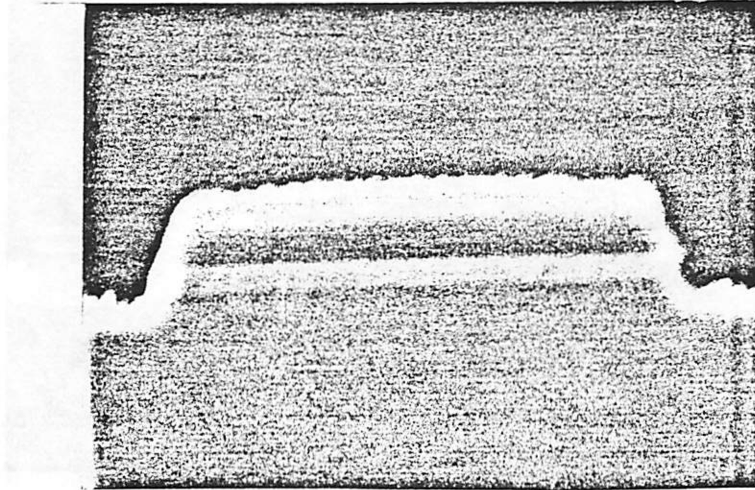

Figure 2. SEM of Etch Sample #1 (11:8 SF_6/CF_2Cl_2)

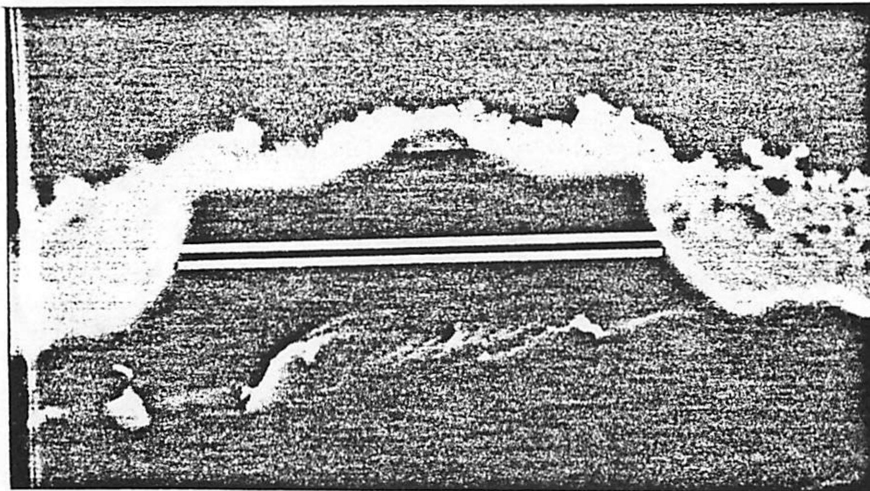

Figure 3. SEM of Etch Sample #2 (16:4 SF_6/CF_2Cl_2)

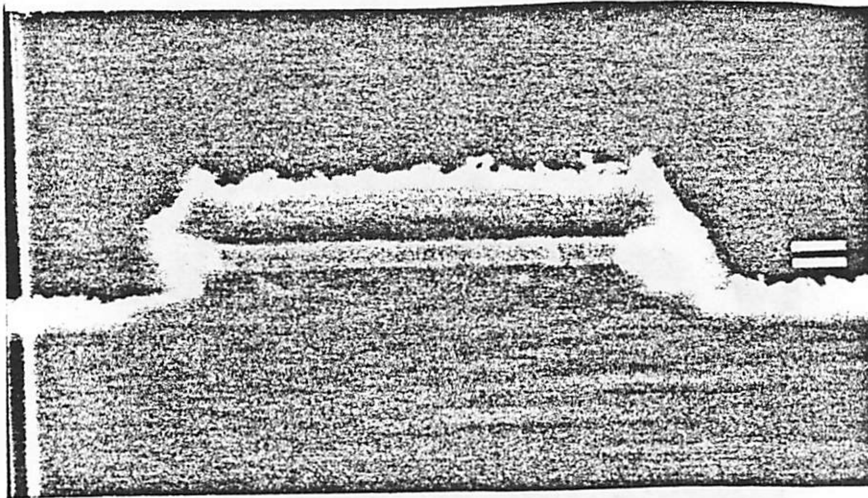

Figure 4. SEM of Etch Sample #3 (6:14 SF_6/CF_2Cl_2)

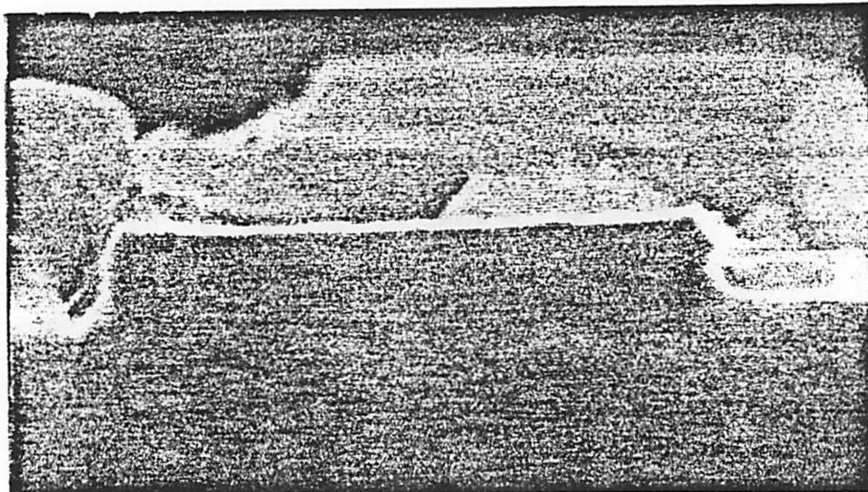

Figure 5. SEM of Etch Sample #4 (11:9 SF_6/CF_2Cl_2)

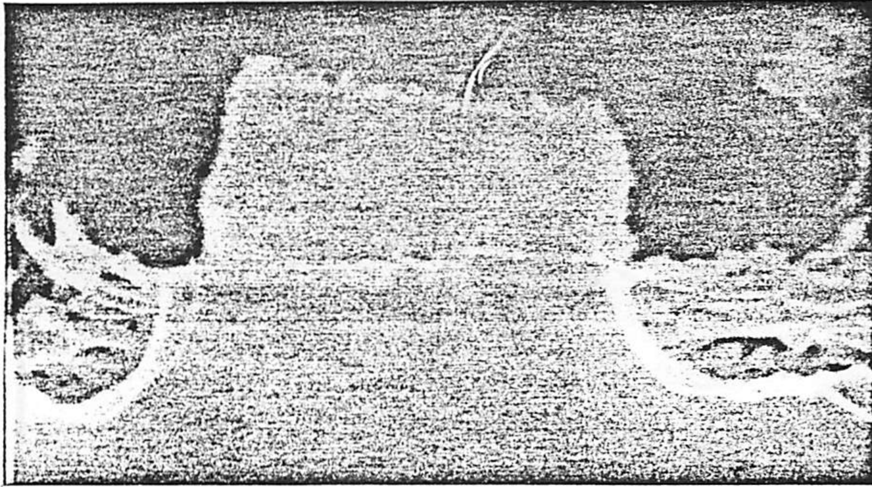

Figure 6. SEM of Etch Sample #5 (12:8 SF_6/CF_2Cl_2)

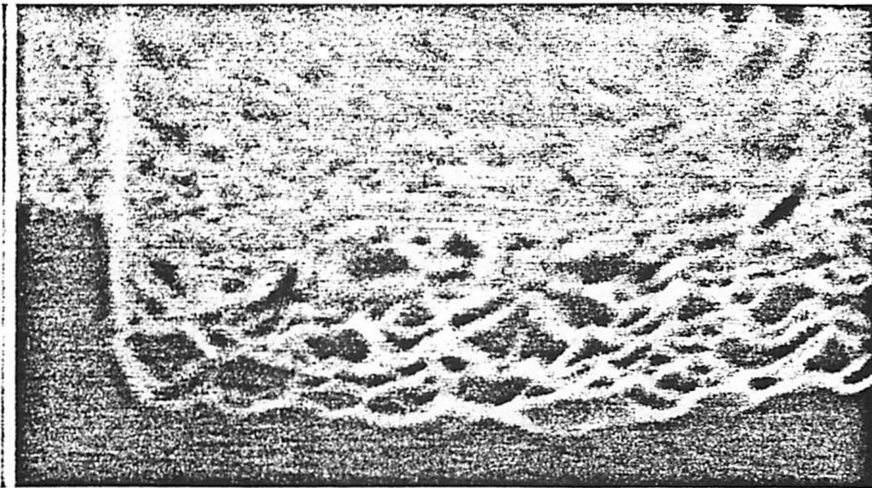

Figure 7. SEM of Etch Sample #5 showing surface roughness

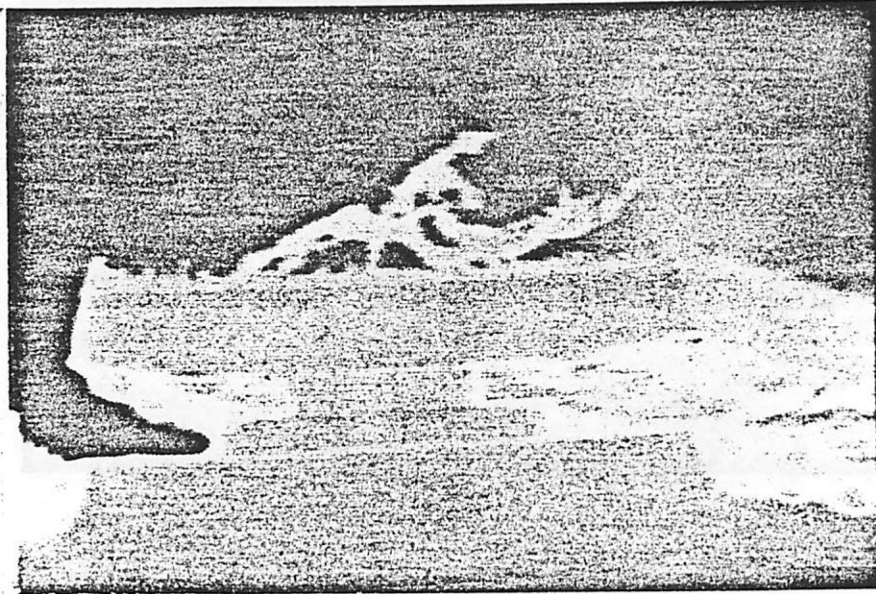

Figure 8. SEM of Etch Sample #6 (13:7 SF_6/CF_2Cl_2)

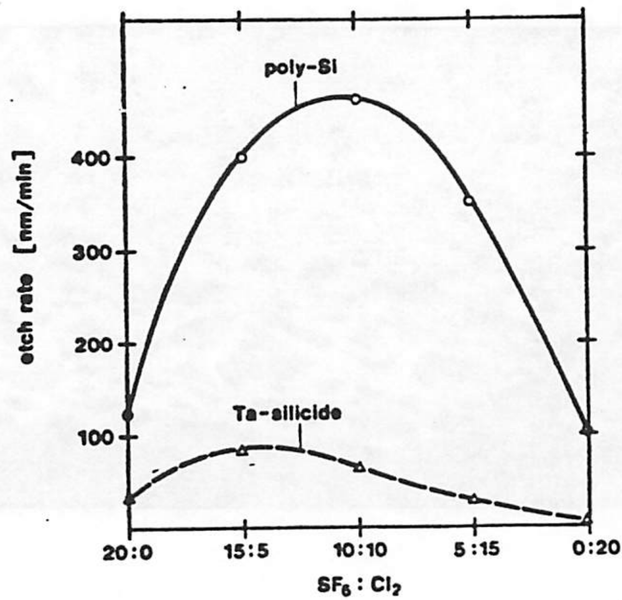

Figure 9. Etch rates versus mixture from Mattausch et al.(Ref 1)

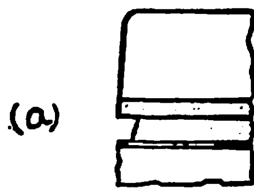

(b)

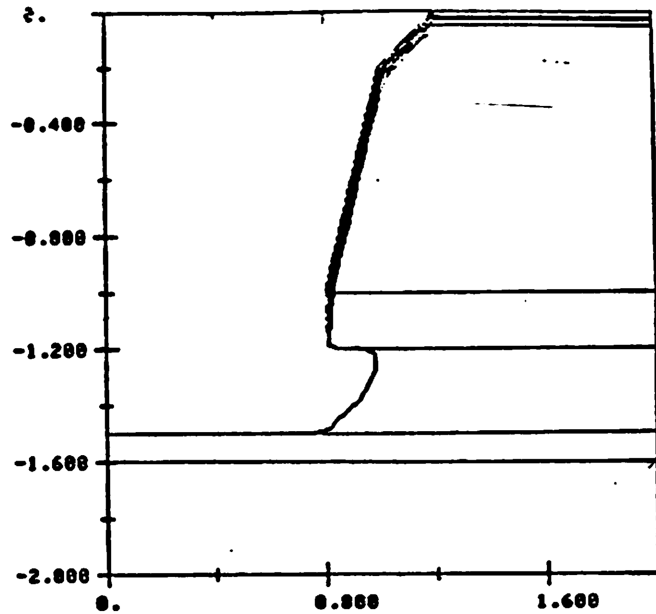

Figure 10. Comparison of literature profile versus simulated profile

For 15:5 SF_6/Cl_2

(a) Literature profile, (b) SAMPLE profile

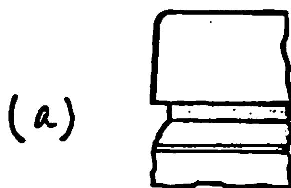

(b)

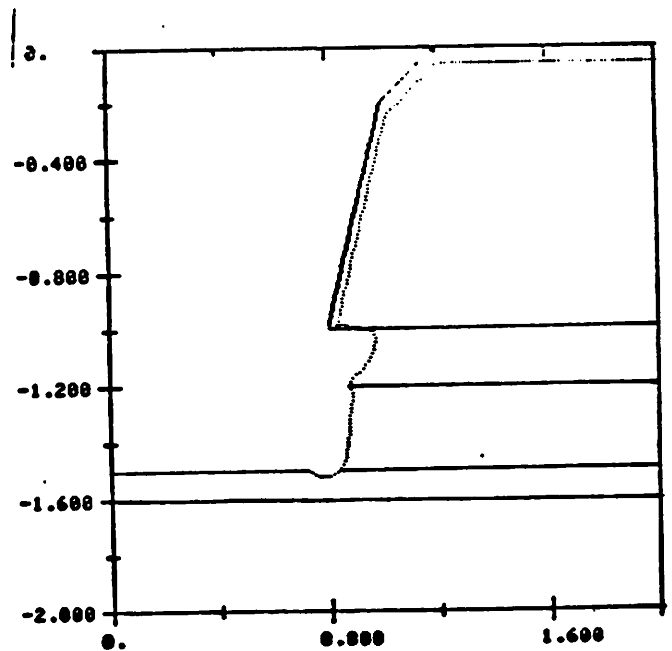

Figure 11. Comparison of literature profile versus simulated profile

For 12.5:7.5 SF_6/Cl_2

(a) Literature profile, (b) SAMPLE profile

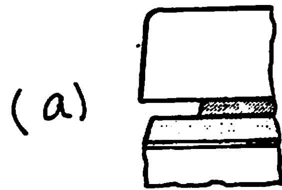

(b)

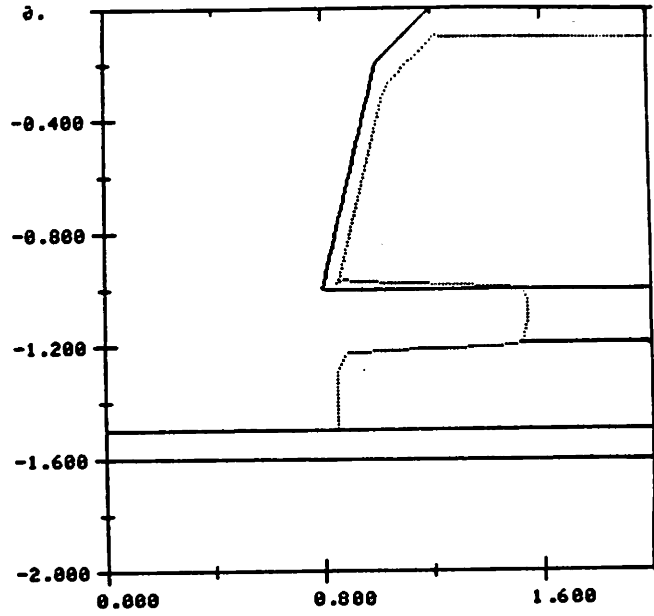

Figure 12. Comparison of literature profile versus simulated profile

For 10:10 SF_6/Cl_2

(a) Literature profile, (b) SAMPLE profile

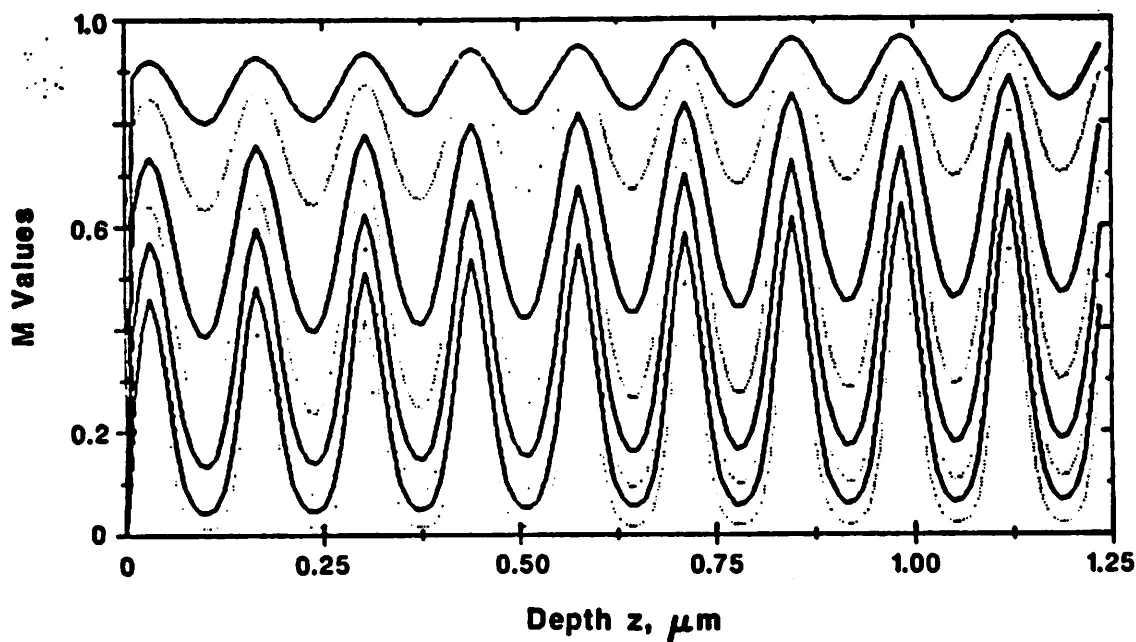

Figure 13. SAMPLE simulation of M distribution for exposure intensities of 12.5 - 200 mJ/cm², for Kodak 820 photoresist.

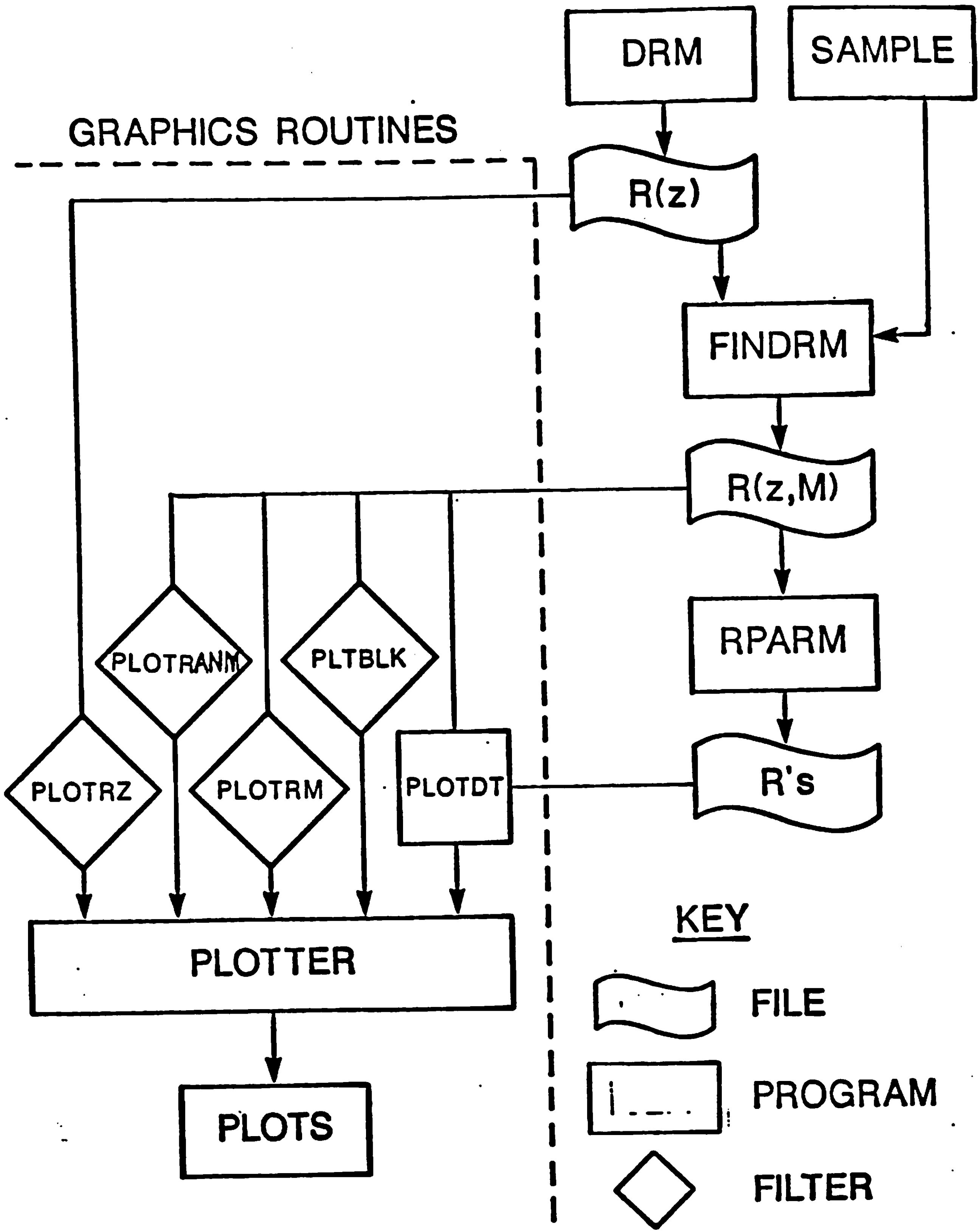

Figure 14. Flow graph of PAREX software suite, showing flow of data through analysis, and graphics filters to view the data.

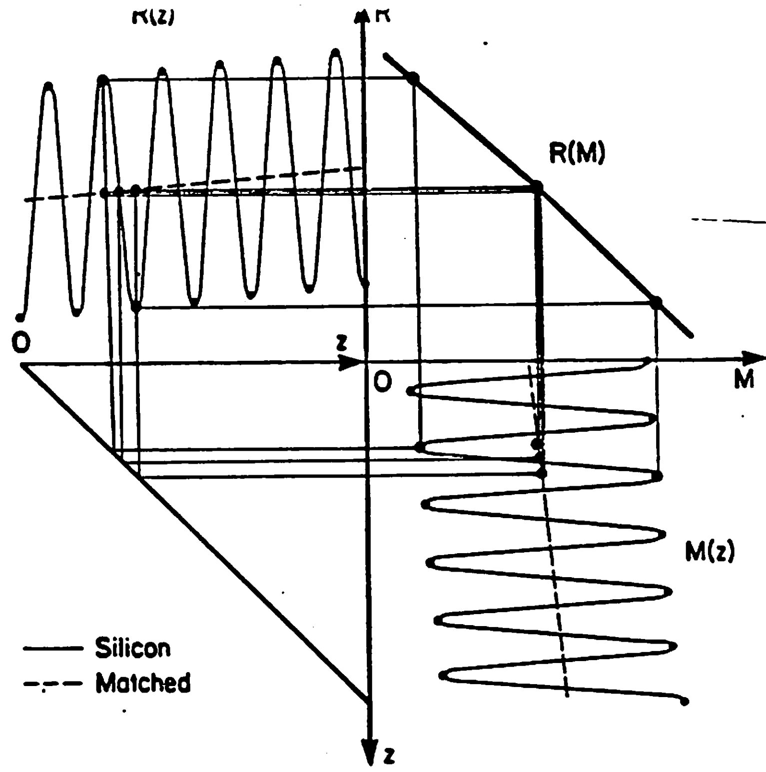

Figure 15. Matching of dissolution rates and M values on reflecting substrates.

Rate vs M Values

Rate (μm/sec)

0.1
0.01
0.001

0
0.1
0.2
0.3
0.4
0.5
0.6
0.7

M (percent of PAC remaining)

0.935 μm
0.950 μm
0.965 μm

Figure 16. Rate versus M values for differing distributions of M versus depth.

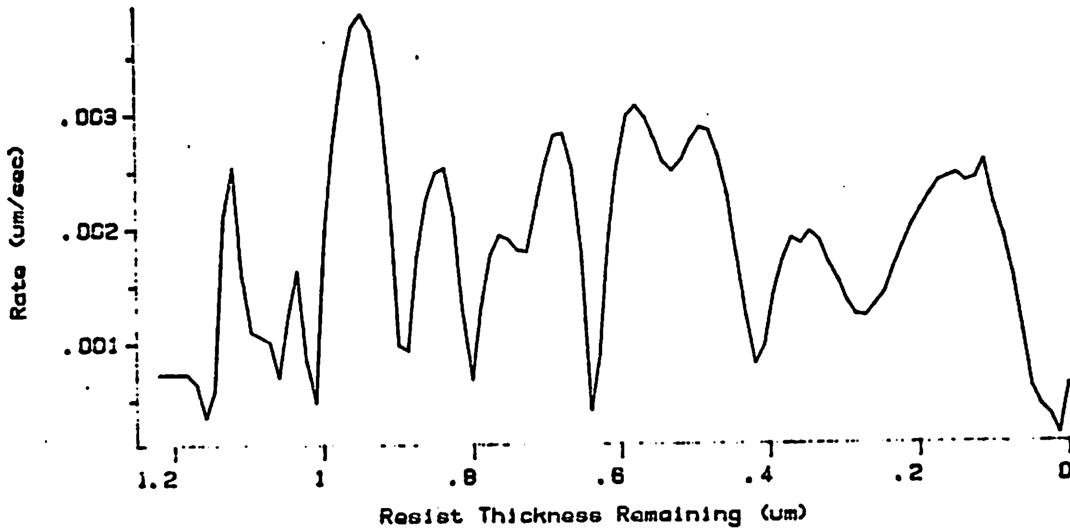

Figure 17. Rate versus thickness taken from DRM (PROSIM). Kodak 820/809 developer.

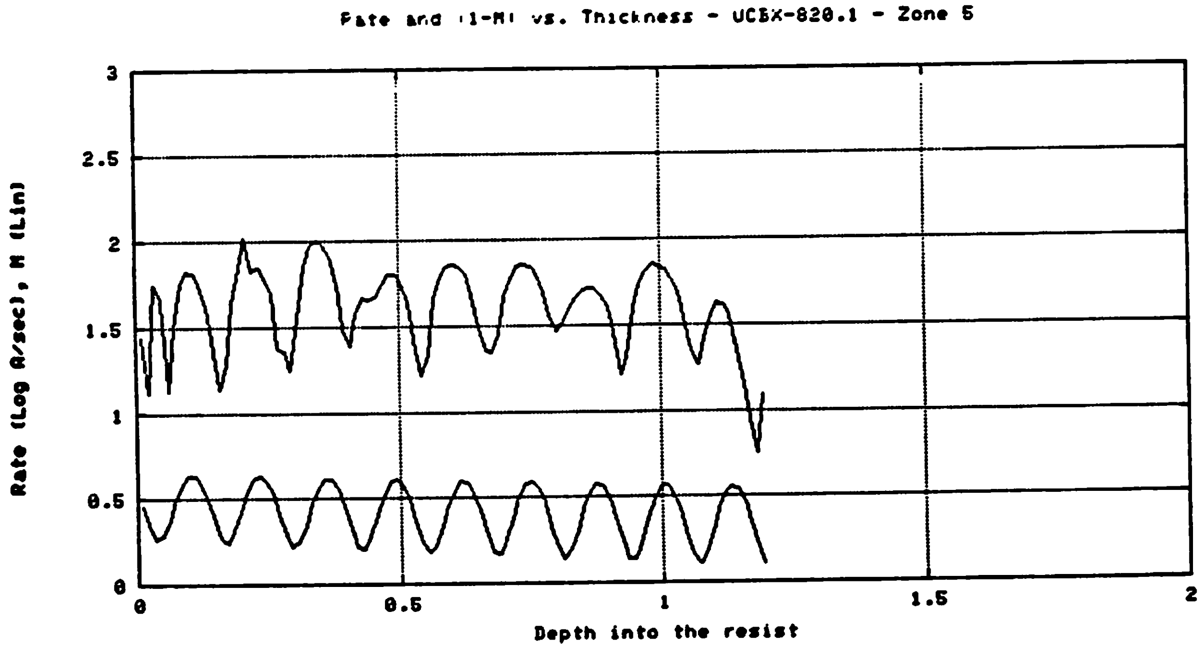

Figure 18. Rate and M versus depth showing matching of period using n_{eff} technique.

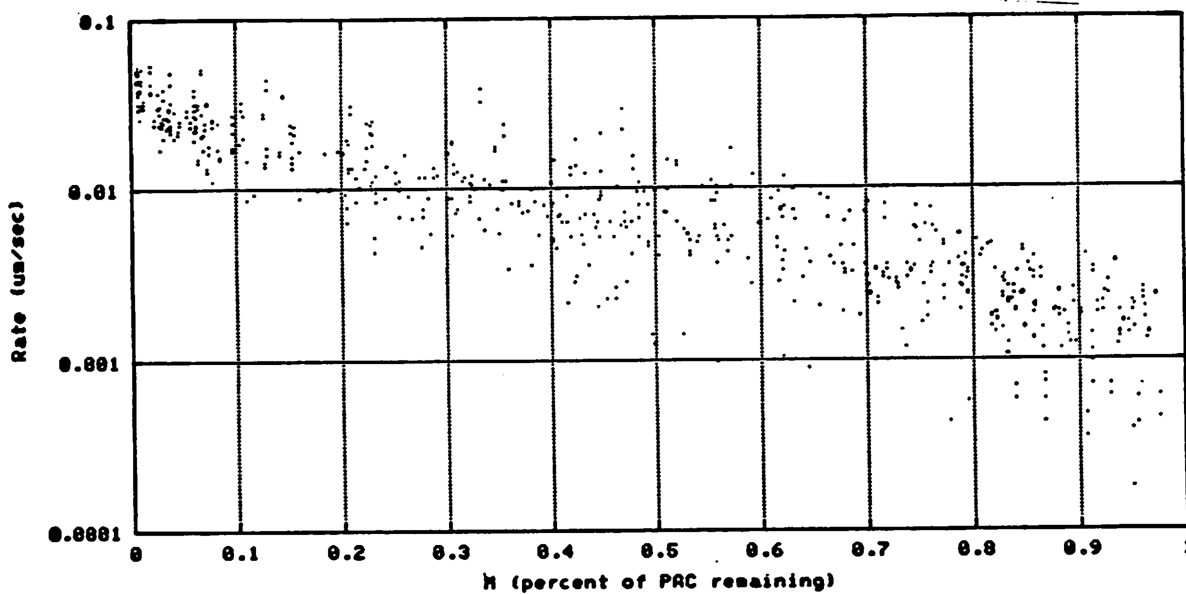

Figure 19. Rate versus M, bulk values only.

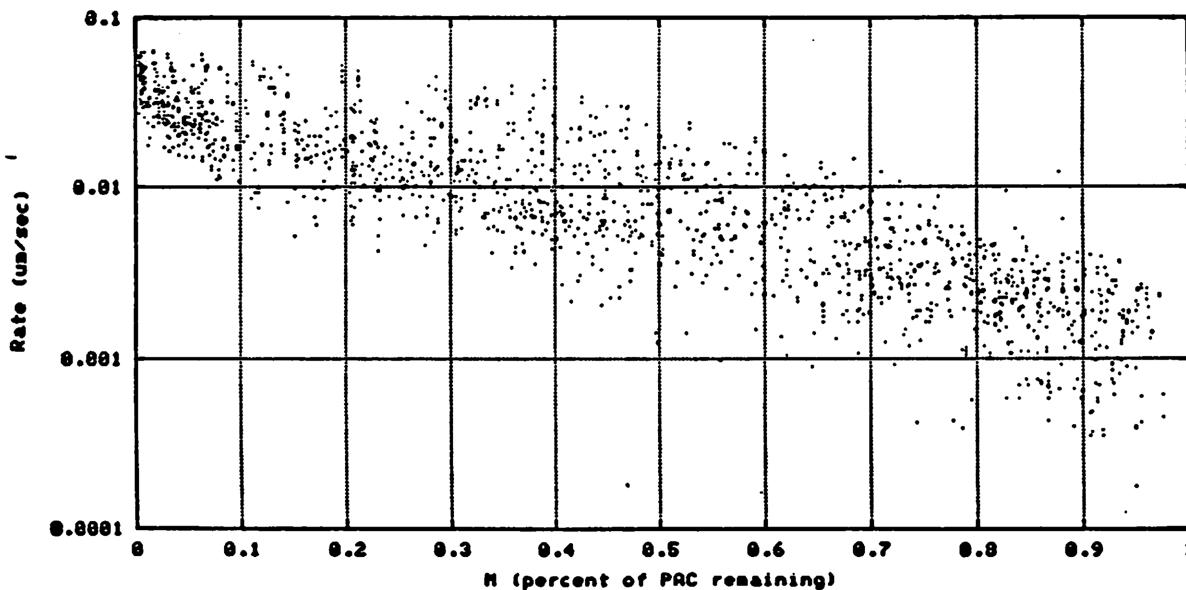

Figure 20. Rate versus M, all data points.

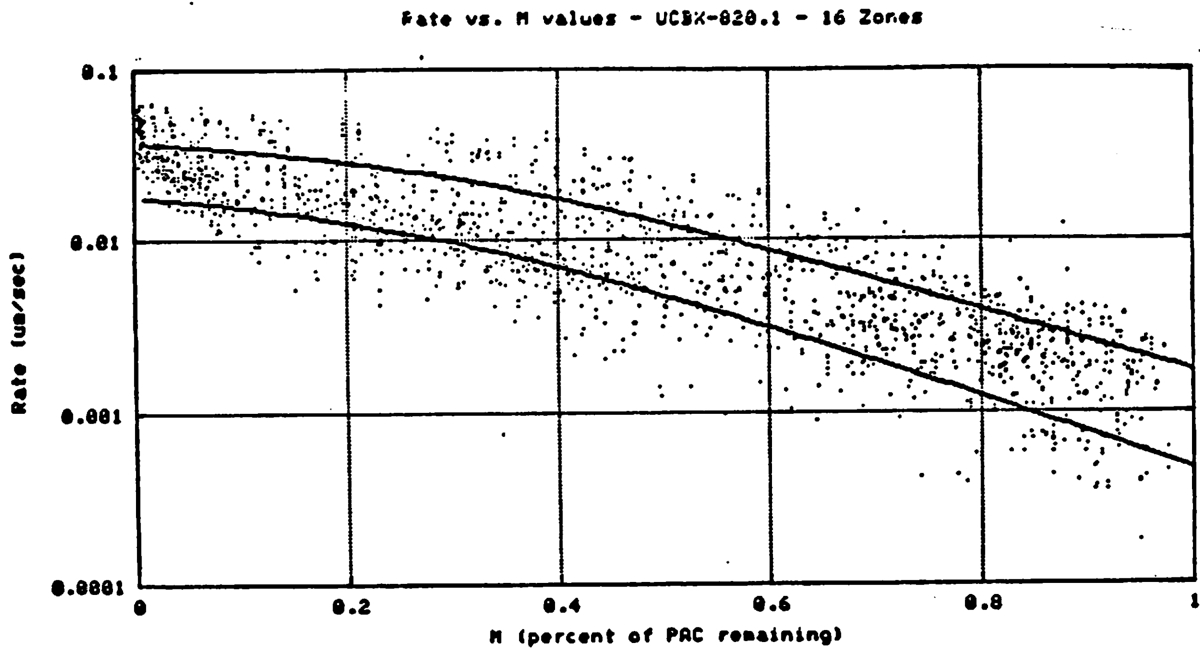

Figure 21. Rate versus M, showing the match of extracted parameters to the experimental data.

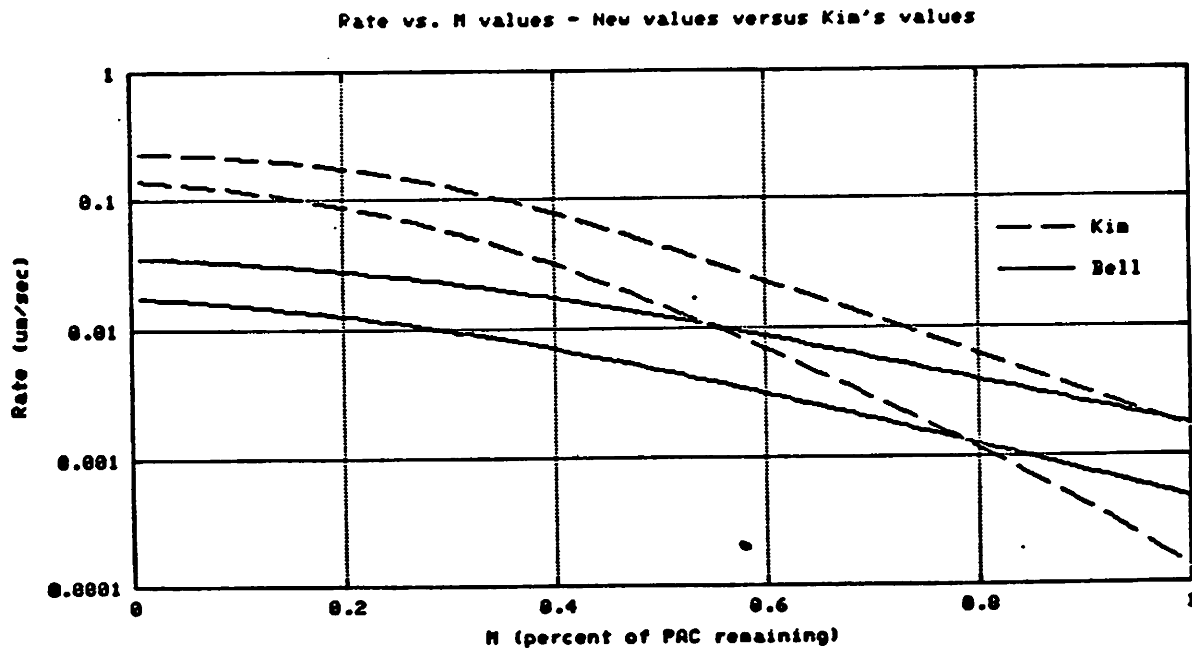

Figure 22. Rate versus M, comparing the extracted parameters and previous literature values.